



Magnetically separable mixed metal oxide nanocomposite (Pd/MnFe₂O₄) for Suzuki cross-coupling in aqueous medium

Damodar J. Sutar^a, Sunil N. Zende^{b,*}, Abhijit N. Kadam^{c,d}, Mukund.G. Mali^e, Pradeep M. Mhaldar^a, Asmita.S. Tapase^f, Chinna Bathula^g, Sang-Wha Lee^c, Gavisiddappa S. Gokavi^{a,*}

^a Department of Chemistry, Shivaji University, Kolhapur, Maharashtra 416004, India

^b Department of Chemistry, Doodhsakhar Mahavidyalaya, Bidri, Kagal, Kolhapur, Maharashtra 416208, India

^c Department of Chemical and Biological Engineering, Gachon University, 1342 Seongnam-aero, Sujung-gu, Seongnam-si, Gyeonggi-do 461-701, Republic of Korea

^d Department of Chemistry, Wilson College(Autonomous), Mumbai, Maharashtra 400007, India

^e School of Chemical Sciences, Panyashlok Ahilyadevi Holkar Solapur University, Solapur, Maharashtra 413255, India

^f Department of Chemistry, Vivekanand College (Autonomous) Kolhapur, Maharashtra 416003, India

^g Division of Electronics and Electrical Engineering, Dongguk University-Seoul, Seoul 04620, Republic of Korea

ARTICLE INFO

Article history:

Received 16 July 2022

Revised 14 September 2022

Accepted 19 October 2022

Available online 23 October 2022

Keywords:

Nanocomposite

Pd/MnFe₂O₄

Suzuki coupling

Aqueous medium

Magnetically separable

ABSTRACT

Magnetically separable Pd/MnFe₂O₄ nanocomposite has been synthesized by coupling palladium with MnFe₂O₄ via citrate gel auto combustion and deposition precipitation method. The physicochemical and microscopic study of Pd/MnFe₂O₄ was investigated using various characterization techniques. The zeta potential of the prepared nanocomposite Pd/MnFe₂O₄ was found to be highly negative value of -36.7 mV, which stabilizes the particle in its dispersed state and also helps to polarize the aryl-halide bond. The catalytic activity of Pd/MnFe₂O₄ was explored for Suzuki cross-coupling of aryl boronic acids and aryl halides (I, Cl, Br) in an aqueous medium. Interestingly, the rate of the slow oxidative addition step of the reaction is enhanced due to the high negative surface charge of the catalyst. It is worth mentioning that high turnover number (TON) and turnover frequency (TOF), thermal stability, ease of handling, nontoxic, magnetically separable, and recyclable are the remarkable properties of the present catalyst. Moreover, the protocol was found to be significant with respect to reaction time, substrate scope, the yield of products, and solvent used for the reaction.

© 2022 Elsevier B.V. All rights reserved.

1. Introduction

Palladium-catalyzed Suzuki cross-coupling for the construction of biaryl units via carbon-carbon (C-C) bond formation is a versatile route in organic synthesis [1]. Although homogeneous palladium catalysts have been widely utilized, they suffer shortcomings such as expensiveness, difficulty in separation from the products, and less efficient cyclization, making them unsuitable for industrial applications [2]. On the other hand, the use of catalysts in the heterogeneous form helps to reduce some of the above-mentioned drawbacks and even leads to remarkable properties. Solid materials [3] such as carbon structures, [4] polymers, [5] and mesoporous silica [6] have been employed as support for palladium catalyst in the synthesis of substituted biaryls from different aryl halides

and phenylboronic acids [7]. Further, owing to the importance of Suzuki cross-coupling efforts are being made for the development of green methodologies with reduced reaction time, higher yield, better substrate scope, and catalyst sustainability.

Nanohybrids, a mixed metal oxide material, are preferably used in catalysis due to their attractive photocatalytic [8–10], electronic [11] and magnetic properties [12]. They are more efficient in solar energy applications [13–17] as a result of increased surface area, stability, reusability, and better dispersion [18]. The advantage of ferrite-supported catalysts is their separation by an external magnet from the reaction mixture avoiding tedious cross-flow filtration and centrifugation [19].

Metal-ferrites MFe₂O₄ (M = Mn, Co, Zn, Mg, Ni, etc.) are eminent cubic spinel materials where oxygen forms a face-centered cubic close packing, and metals occupy either tetrahedral or octahedral interstitial sites [20]. Among the ferrites, manganese ferrites (MnFe₂O₄) are a group of soft spinel ferrite materials with high magnetization, more chemical stability, and special opti-

* Corresponding authors.

E-mail addresses: sunil.zende018@gmail.com (S.N. Zende), gsg_chem@unishivaji.ac.in (G.S. Gokavi).

cal property [21] due to which they are used for high-density magnetic recording, ferrofluid technology, electronic devices, magnetic resonance imaging (MRI), microwave adsorption and environmental analysis [22,23]. They also find applications as catalyst support in regio- and stereoselective synthesis of oxazolidin-2-ones [24], tetrahydrobenzo[b]pyran & indazolo[2,1-b] phthalazine-triones [25], oxidation of organic pollutants [26], photocatalytic water-splitting [27] and degradation of organic dyes [28].

Various ligands for palladium have been utilized to increase the catalytic efficiency of the Suzuki-Miyaura coupling reaction. The phosphine ligands coordinated to the Pd(0) are electron rich thus facilitating all the three steps involved in Suzuki Miyaura coupling reactions [29]. Since the phosphorous-containing ligands are air and moisture sensitive more recently nitrogen-containing ligands like N-heterocyclic carbenes were replaced by phosphorus-containing ligands [30]. In both, the ligands used it has been noticed that the electron-rich nature of the ligand plays an important role in the catalysis. In the case of solid and magnetically separable nanocatalysts, the surface charge is also helpful in increasing the catalytic efficiency which can be understood by measuring the zeta potential of the catalyst. Further, the dispersion stability of nanoparticles depends upon their surface charge [31–33] which prevents the particles to aggregate. The more the surface charge greater will be the dispersion stability. Therefore, we explored the synthesis of palladium coated on MnFe_2O_4 supported composite via citrate gel auto combustion and deposition precipitation method and its catalytic application for Suzuki cross-coupling in an aqueous medium.

2. Materials and methods

2.1. Materials and characterization

Aryl halides, and Phenyl boronic acids (Sigma-Aldrich), were utilized as received. Reagent grade iron (III) citrate [$\text{C}_6\text{H}_5\text{FeO}_7$], manganese nitrate [$\text{Mn}(\text{NO}_3)_2 \cdot 4\text{H}_2\text{O}$], citric acid anhydrous [$\text{C}_6\text{H}_8\text{O}_7$], polyvinyl pyrrolidone (PVP), ammonia (NH_3) and K_2CO_3 were used as received. The melting points of synthesized derivatives were recorded by an open capillary method and are uncorrected. NMR spectra were recorded on Bruker 400 MHz spectrometer (Irradiation frequency: 400 MHz for ^1H NMR and 100 MHz for ^{13}C NMR) in CDCl_3 using TMS as an internal standard while δ values are expressed in ppm. The crystallographic phase and structural evidence were confirmed by employing an X-ray diffraction technique (D/max-2200 pc, Rigaku, Japan) using $\text{Cu K}\beta$ source of radiation, Hitachi S-4700 SEM instrument was used to investigate the surface morphology of samples. The S-Twin AP Tech., G2mF30, 200 kV Tecnai, USA, was used to perform TEM. The surface area of synthesized nanocomposite and its zeta potential was determined by using BET (Quanta chrome NOVA 1000e, USA) and Particle size analyzer and Zeta potential (Malvern-UK, Nano ZS90).

2.2. Synthesis of nano crystalline MnFe_2O_4

The crystalline MnFe_2O_4 support has been synthesized by the citrate-gel auto combustion method [34]. The stoichiometric quantities of iron citrate and manganese nitrate were dissolved separately in a minimum amount of deionized water and mixed together with constant stirring. The equimolar amount of citric acid was added to the above mixture to get a metal-citrate precursor followed by addition of polyvinyl pyrrolidone (PVP) as a capping agent with constant stirring. The pH of the solution was adjusted to 9–9.5 by dropwise addition of ammonia solution. The resultant sol was heated at 80°C for 3 h to obtain brown agglomerates of

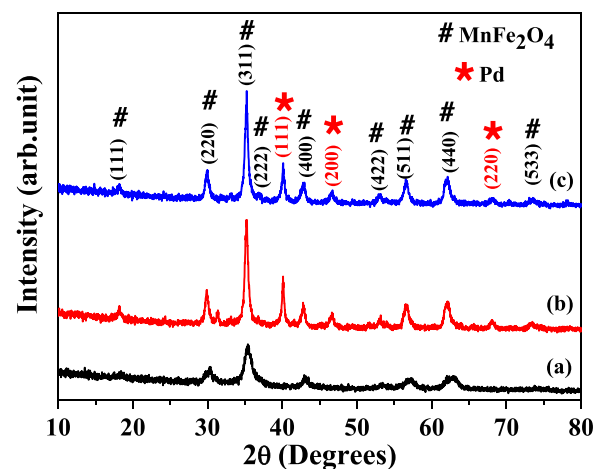


Fig. 1. X-ray diffraction patterns of (a) MnFe_2O_4 NPs. (b) Reused Pd/ MnFe_2O_4 nanocomposite (c) Fresh Pd/ MnFe_2O_4 nanocomposite.

MnFe_2O_4 nanoparticles. The MnFe_2O_4 nanoparticles were crushed and sintered at 300°C for 2 h.

2.3. Synthesis of Pd/ MnFe_2O_4 nanocomposite

The palladium immobilized MnFe_2O_4 nanocomposite was prepared by the deposition-precipitation method [35]. All the procedures were carried out under sonication. Initially, MnFe_2O_4 (1 g) was dispersed in ethanol (30 mL) for 30 min followed by the addition of 150 mg of PdCl_2 upon continuing sonication for another 30 min. Finally, 3 mL of $\text{NH}_2\text{NH}_2 \cdot \text{H}_2\text{O}$ was added dropwise to the above mixture followed by sonication for 30 min. The prepared catalyst was simply separated by an external magnet and washed with distilled water and ethanol. The resultant nanocomposite was dried under a vacuum and 30 mg of the catalyst is used for the Suzuki cross-coupling reaction. The amount of Pd loaded on MnFe_2O_4 is 0.01483 mmol per 30 mg of MnFe_2O_4 . This loading of Pd can be varied by varying the amount of PdCl_2 added after dispersion of MnFe_2O_4 in ethanol. The catalyst MnFe_2O_4 is reported to be superparamagnetic as studied by VSM curves [36].

2.4. General procedure for Suzuki cross-coupling

A mixture of aryl halide (1 mmol), aryl boronic acid (1.2 mmol), K_2CO_3 (2 mmol), and 30 mg of Pd/ MnFe_2O_4 catalyst (1.5 mol% of Pd) was added to 25 mL round bottom flask containing 4 mL DMF: Water (1:1). The reaction mixture was refluxed and the progress of the reaction was analyzed by TLC (petroleum ether: ethyl acetate 9:1). Upon completion of the reaction, the catalyst was separated by an external magnet and the reaction mixture was extracted with ethyl acetate (3×5 mL). The combined extract was dried over anhydrous Na_2SO_4 and evaporated under reduced pressure. Finally, the crude product was purified by column chromatography (petroleum ether-ethyl acetate, 9:1). The final product was analyzed by ^1H and ^{13}C NMR spectroscopy.

3. Result and discussion

3.1. Characterization of the catalyst

The crystal structure and phase purity of as-synthesized pristine MnFe_2O_4 and Pd/ MnFe_2O_4 nanocomposite (before and after use) were confirmed by X-ray diffraction patterns (Fig. 1). The XRD pattern of MnFe_2O_4 (Fig. 1a) exhibits peaks at 2θ values of 30.31° , 35.30° , 35.8° , 43.03° , 53.38° , 56.94° , 62.97° , 73.89° corresponding to the (111), (220), (311), (222), (400), (422), (511),

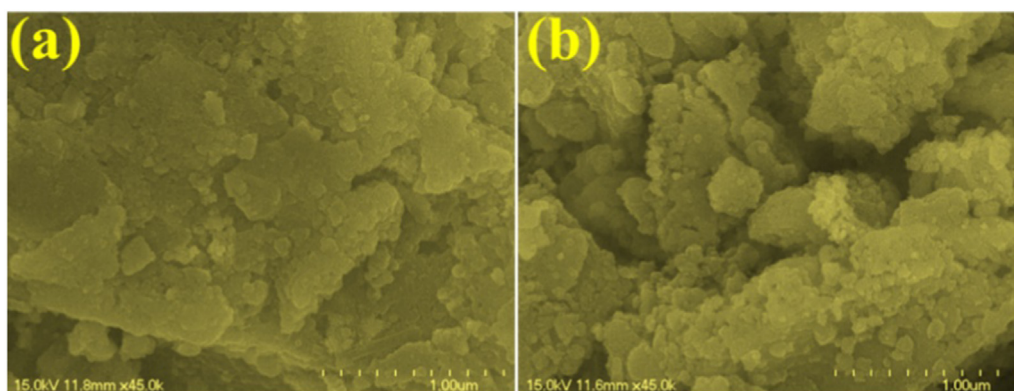


Fig. 2. SEM images of (a) MnFe₂O₄ nanosheets, (b) Pd/MnFe₂O₄ nanocomposite.

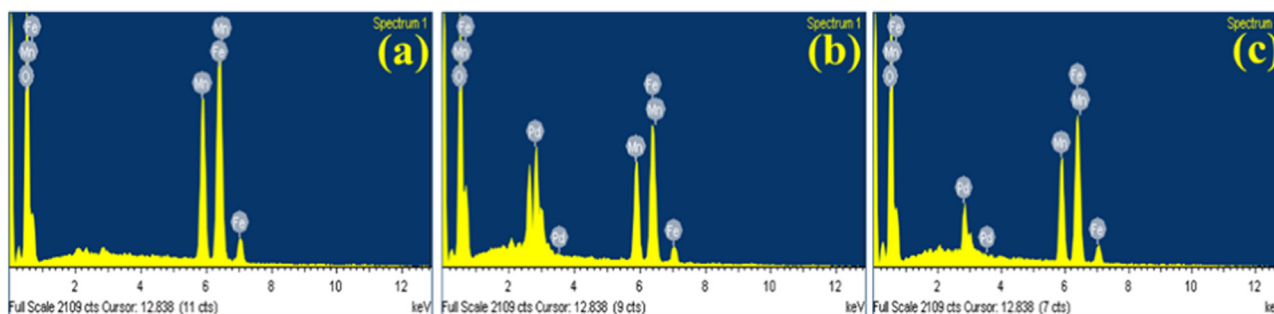


Fig. 3. EDX spectrum of (a) MnFe₂O₄ nanoparticles, (b) Pd/MnFe₂O₄ nanocomposite (fresh), (c) Pd/MnFe₂O₄ nanocomposite (after use).

(440), and (533) crystal planes, respectively. All diffraction peaks matched well with the cubic spinel structure of MnFe₂O₄ (JCPDS card no. 73–1964). Furthermore, no additional peaks due to impurities or other phases appeared, suggesting the phase purity of the MnFe₂O₄. In the XRD pattern of Pd/MnFe₂O₄ nanocomposite (Fig. 1c), the additional diffraction peaks originated at 2θ values of 40.08°, 46.64°, and 68.09° assigned to (111), (200), (220) lattice planes of face-centered cubic (fcc) crystal structure (JCPDS card no. 46–1043) of palladium, respectively, confirming the successful fabrication of palladium coated on MnFe₂O₄. From X-ray diffraction peaks, the average crystallite size was calculated using Scherrer's formula, $L = 0.9 \lambda / \beta \cos \theta$, where, symbols have their usual meaning. The average crystallite sizes of MnFe₂O₄ and Pd/MnFe₂O₄ were found to be around 6.9 nm and 14.5 nm respectively. The XRD pattern of the used Pd/MnFe₂O₄ catalyst (Fig. 1b) exhibited identical diffraction peaks to those of a fresh catalyst, indicating that its crystallinity was unchanged even after several cycles. This result confirms the structural integrity of recycled Pd/MnFe₂O₄ catalyst, suggesting its practical application.

The surface morphology of bare MnFe₂O₄, and Pd/MnFe₂O₄ nanocomposite was investigated by scanning electron microscope technique (Fig. 2). The SEM image of MnFe₂O₄ confirms the formation of nanosheets (NSs) like morphology, which providing abundant active sites for the growth of palladium NPs (Fig. 2a). The Pd/MnFe₂O₄ nanocomposite also possessed nanosheets like morphology with evenly embedded palladium NPs (Fig. 2b). Thus, SEM images manifested successfully fabrication of Pd NPs embedded with 2D nanosheets of MnFe₂O₄.

The elemental composition and purity of as-prepared catalysts were confirmed by EDS analysis. EDS spectrum of MnFe₂O₄ NSs, fresh and reused Pd/MnFe₂O₄ nanocomposite are depicted in (Fig. 3). The presence of Mn (22.40%), Fe (35.43%), and O (42.17%) confirm the formation of MnFe₂O₄ with high purity. The EDS spectrum of Pd/MnFe₂O₄ indicates the presence of Pd with 5.24 weight percent, which revealed the uniform dispersion of Pd over the sur-

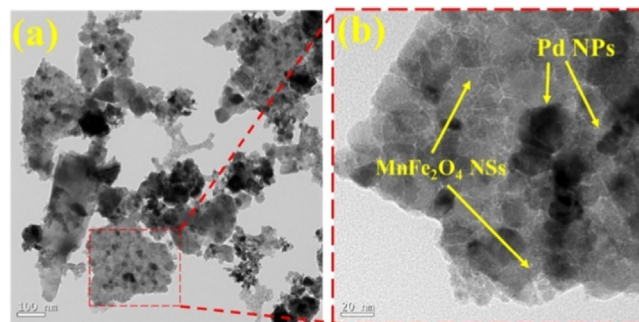


Fig. 4. (a) and (b) TEM micrographs of Pd/MnFe₂O₄ nanocomposite with different magnifications.

face of the MnFe₂O₄ nanocomposite. The elemental composition of reused Pd/MnFe₂O₄ catalyst was found to be nearly the same compared to that of the fresh catalyst. Although the reduction in the amount of Pd confirms leaching, the efficiency of the catalyst is not altered significantly.

The detailed insight into the morphology of synthesized Pd/MnFe₂O₄ composites was further examined by TEM analysis with different magnifications. The resulting micrographs were depicted in Fig. 4. The TEM images clearly reveal that the roughly spherical morphology of Pd NPs embedded in 2D nanosheets of MnFe₂O₄. The deposition of palladium (depicted by dark) on the surface of MnFe₂O₄ nanosheets can be clearly seen in the TEM image, which is in good agreement with SEM. Thus, the fabrication of Pd/MnFe₂O₄ nanocomposites was confirmed by XRD, SEM, TEM, and EDS analysis.

It is fact that the surface area of the catalyst play a significant role in its catalytic efficiency. The BET study was performed to investigate the surface area of synthesized Pd/MnFe₂O₄ nanocomposite. Nitrogen adsorption-desorption curves for Pd/MnFe₂O₄ cat-

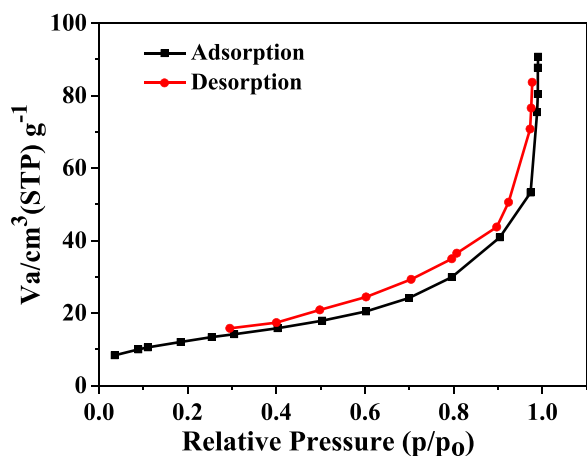


Fig. 5. Nitrogen adsorption-desorption isotherm of Pd/MnFe₂O₄ nanocomposite.

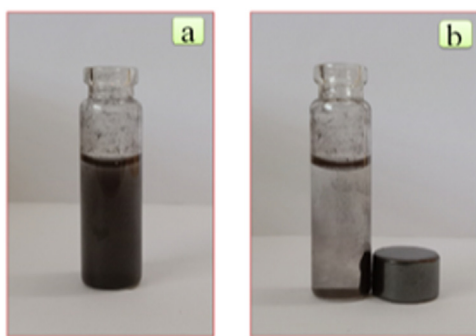


Fig. 6. Magnetic property of nanocomposite (a) dispersed in the reaction mixture, and (b) Magnetic separation of the catalysts from the reaction medium.

alyst are depicted in Fig. 5. The Pd/MnFe₂O₄ catalyst exhibited type III isotherm, suggesting its mesoporous nature. The surface area of synthesized nanocomposite was found to be 44.79 m² g⁻¹, which confirms the presence of a large active site for efficient catalytic activity.

The superparamagnetic [36] character of the synthesized Pd/MnFe₂O₄ was verified by placing a horse-shoe magnet near the reaction mixture. The Pd/MnFe₂O₄ nanocomposite is separated completely and accumulates near the magnet [37,38] and the corresponding photograph is shown in Fig. 6.

3.2. Catalytic activity

After a detailed analysis of the Pd/MnFe₂O₄ nanocomposite, we employed it for Suzuki cross-coupling of aryl halide and aryl boronic acid to furnish substituted biaryls (Scheme 1). Initially, we focused on the optimization of reaction conditions with respect to solvent, base, reaction time, and amount of catalyst.

A model reaction of iodobenzene, phenylboronic acid and K₂CO₃ base at reflux condition has been selected for the screening of solvents. Initially, the model reaction was performed in water which furnished a 44% yield of the desired product (Table 1, Entry 1). The solvents like toluene, ethanol, and DMSO were also employed resulting in moderate yields (Table 1, Entries 2–4). DMF provided a sufficient yield of biphenyl in two hours (Table 1, Entry 5). Considering the improved yield in DMF, a mixed solvent system (ethanol: water and DMF: water) has been employed for the model reaction (Table 1, Entries 6–9). Interestingly 98% of an admirable yield of desired product was obtained for DMF: water (1:1) (Table 1, Entry 7).

Table 1
Optimization of solvent for Suzuki cross coupling^a.

Entry	Solvent	Time (min)	Yield ^b (%)
1	H ₂ O	300	44
2	Toluene	140	70
3	Ethanol	120	76
4	DMSO	120	60
5	DMF	120	80
6	Ethanol/H ₂ O (1:1)	60	78
7	DMF/H₂O (1:1)	10	98
8	DMF/H ₂ O (3:2)	30	82
9	DMF/H ₂ O (7:3)	30	78

^a Reaction conditions: Iodobenzene (1.0 mmol), phenylboronic acid (1.2 mmol), K₂CO₃ (2.0 mmol), solvent (4 mL) and catalyst (1.5 mol% of Pd), reflux. ^b Isolated yield.

Table 2
Effect of temperature on Suzuki cross-coupling^a.

Entry	Temperature (°C)	Time (min)	Yield ^b (%)
1	RT	120	52
2	50	90	84
3	60	60	82
4	70	30	88
5	80	30	92
6	90	10	98
7	100	10	98

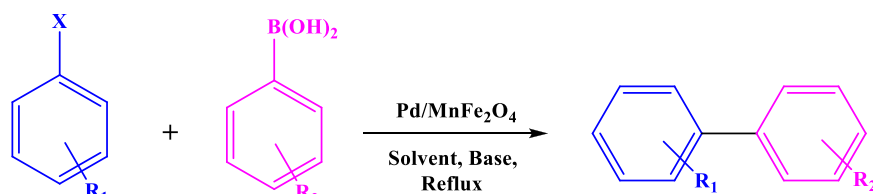
^a Reaction conditions: Iodobenzene (1.0 mmol), phenylboronic acid (1.2 mmol), K₂CO₃ (2.0 mmol), solvent (4 mL) and 30 mg of catalyst (1.5 mol% of Pd), reflux. ^b Isolated yield.

3.2.1. Effect of various bases and temperature

Considering DMF: H₂O (1:1) as a suitable solvent, a screening of various bases has been carried out for the same model reaction. The result for the optimization study of the base is depicted in Fig. 7. Different organic and inorganic bases viz. K₂CO₃, NaOH, TEA, Na₂CO₃, and NaHCO₃ were tested for Suzuki cross-coupling. Among these, K₂CO₃ as a base resulted in a high yield of the desired product (98%) in 10 min only. The other bases gave low to moderate yield for one hour.

Effect of temperature for model reaction in presence of K₂CO₃ and DMF: H₂O (1:1) solvent has been investigated (Table 2). Initially, the reaction was performed at room temperature resulting in a 52% yield in 2 h. The model reaction was performed at different temperatures (50 to 100 °C) with 10 °C intervals. Moderate yields are obtained for the reaction at 50 °C to 80 °C. Interestingly 98% yield was observed at 90 °C within 10 min only. Further increase in temperature did not alter the yield which confirmed that 90 °C is the suitable temperature for the reaction. Stepwise analysis of catalyst, optimization of reaction conditions, and screening of different factors revealed that 30 mg of Pd/MnFe₂O₄ catalyst (1.5 mol% Pd), K₂CO₃ as a base, and DMF: H₂O (1:1) solvent are the effective criteria for Suzuki cross-coupling of 1 mmol of aryl halide and 1.2 mmol of aryl boronic acid. The generality of the catalyst for coupling diverse electronically substituted aryl halides and boronic acids

(Table 3) was explored using optimized conditions. Reactions of more reactive aryl iodides (Entries 1–6, Table 3) and aryl bromides (Entries 7–13, Table 3) with substituted / phenyl boronic acids have been performed and high yield of required compounds were produced in a shorter reaction time indicating that the catalyst is effective. Considering the electronic effect of various substituents on aryl halides, it was found that electron-rich groups of aryl bromide furnished high yields in a short reaction time than that of the electron-deficient moieties (Entries 8–12, Table 3). Benzofuran-2-ylboronic acid on coupling with 4-bromo anisole provided 86% yield of heterobiaryls were obtained (Entry 13, Table 3). The cou-



Scheme 1. Suzuki cross-coupling of aryl halides and phenyl boronic acids.

pling of deactivating aryl chlorides was also performed and sufficient yields were obtained in 2–5 h (Entries 14–18, Table 3). The yield of the product of aryl chloride substituted with electron withdrawing group (Entries 14–16, Table 3) is higher than that of the electron donating groups (Entries 17–18, Table 3). Overall, the catalyst was found to be superior for Suzuki cross-coupling of aryl halides (I, Br, Cl) with substituted boronic acids.

3.2.2. Plausible mechanism of Suzuki cross coupling

The Suzuki cross coupling in presence of a catalyst occurs through oxidative addition, transmetalation and reductive elimination. The rate of these Suzuki cross coupling reactions is controlled by the oxidative addition step [39] and the negative charge around the Pd(0) leads to increase in efficiency of the catalyst used. In case of homogeneous palladium catalysts, the electron rich ligands containing phosphorous or nitrogen are more efficient. The solid Pd(0) materials used for photocatalysis such as Au-Pd alloy or an electrode [39] bearing palladium are also possess the negative charge around the palladium metal leading to the enhancement in the rate. Since the oxidative addition of aryl halide (Ar-X) is the rate determining step in Suzuki cross coupling, the in-

crease in negative charge surrounding the Pd(0) polarizes the Ar-X bond, enabling it to break and generate the transition state. The Pd/MnFe₂O₄ nanocomposite catalyst utilized in this study has extremely negative zeta potential values (Table 4), which favours polarization of the Ar-X bond and thus rate of the oxidative addition step. Such an increase in the rate of the slow step of Suzuki cross coupling reaction leads to the greater efficiency of the catalyst. The comparative study of some Suzuki cross coupling reactions reported earlier is also made and the results of the present study also indicate Pd/MnFe₂O₄ nanocomposite is a better catalyst in support of the conclusion.

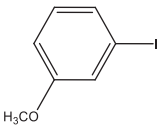

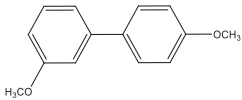
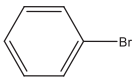
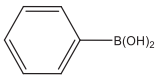
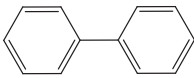
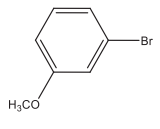
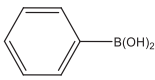
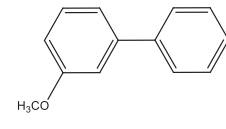
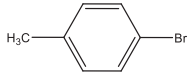
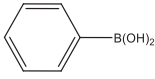
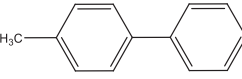
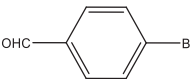
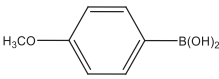
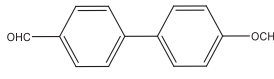
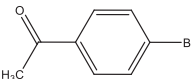
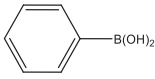
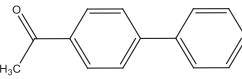
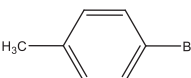
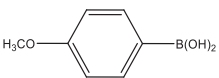
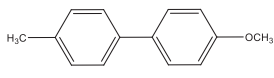
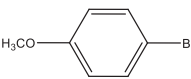
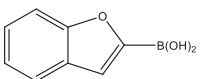
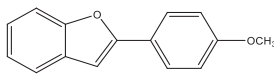
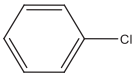
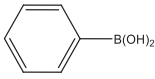
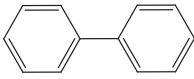
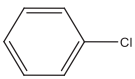
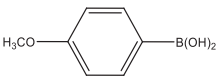
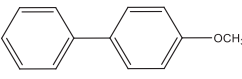
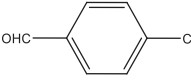
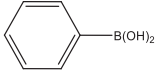
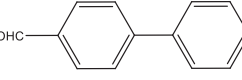
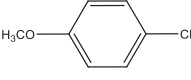
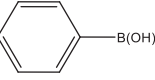
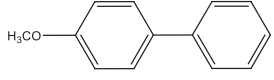
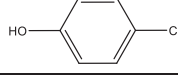
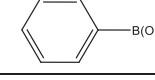
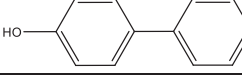
The plausible mechanism for Suzuki cross coupling catalysed by Pd/MnFe₂O₄ nanocomposite was depicted in Scheme 2, involving three steps viz. oxidative addition, transmetalation and reductive elimination. The oxidative addition of aryl halide to Pd⁽⁰⁾/MnFe₂O₄ results in breaking of C-X bond of aryl halide and formation of Pd-Ar and Pd-X bond (Complex 1). Complex 1 under the participating of base (K₂CO₃) reacts with aryl boronic acid furnishes Complex 2 via transmetalation. Complex 2 on reductive elimination gives desired biaryl product and generates Pd⁽⁰⁾/MnFe₂O₄ species for recycle.

Table 3
Pd/MnFe₂O₄ catalyzed Suzuki cross-couplings for substituted biaryl synthesis^{a, b, c}.

Entry	Aryl halide	Phenyl boronic acid	Product	Time (min)	Yield ^b (%)	TON/TOF ^c
1				10	98	6608/660
2				15	95	6405/427
3				10	98	6608/660
4				10	95	6405/640
5				20	80	5394/269

(continued on next page)

Table 3 (continued)

6				10	93	6271/ 627
7				30	96	6473/ 215
8				30	94	6338/ 211
9				30	94	6338/ 211
10				90	82	5529/ 61.43
11				120	78	5259/ 43.83
12				30	96	6473/ 215
13				30	86	5799/ 193
14				120	90	6068/ 50.57
15				90	80	5394/ 59.93
16				180	64	4315/ 23.97
17				240	58	3910/ 16.29
18				270	60	4045/ 14.98

^a Reaction conditions: aryl halide (1.0 mmol), arylboronic acid (1.2 mmol), K₂CO₃ (2.0 mmol), DMF:H₂O (1:1) (4 mL) and catalyst (1.5 mol% of Pd), reflux.

^b Isolated yield.

^c min⁻¹.

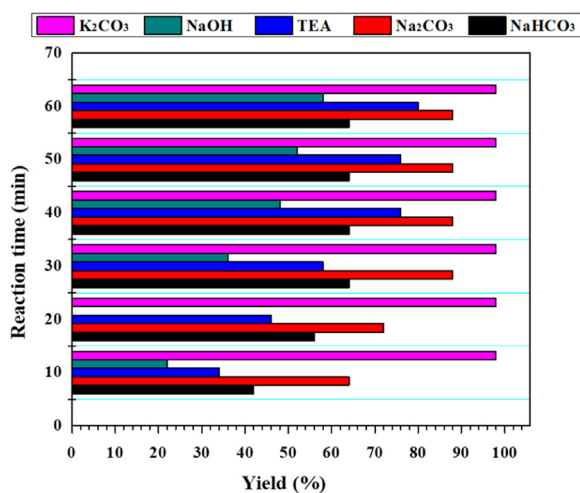
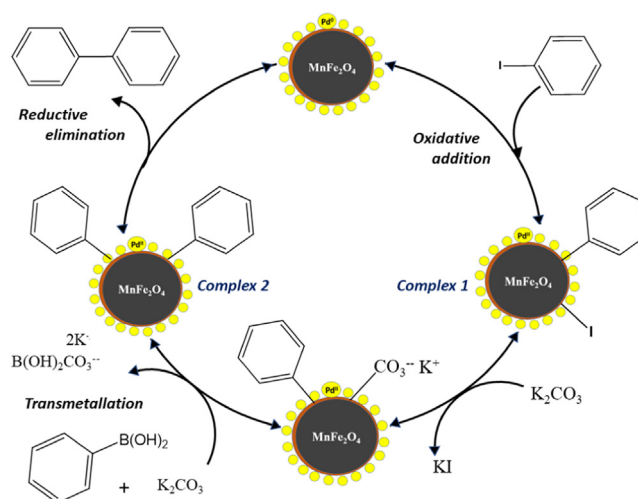
Table 4
Values of zeta potential and particle size of the Pd/MnFe₂O₄ nanocomposite.

Sample	Average Size (nm)	Intensity (%)	Zeta Potential(mV)
Pd/MnFe ₂ O ₄	350.6	100	-36.7
Pd/MnFe ₂ O ₄ after use	315.8	100	-35.6

Table 5

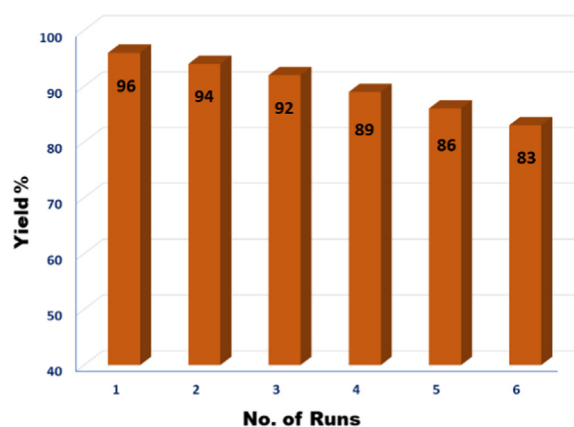
Catalytic performance of different magnetically Pd based nanocomposites in the coupling reaction of iodobenzene and phenyl boronic acid.

Entry	Catalyst	Reaction Conditions	Time (min)	Yield (%)	Ref.
1	Pd@Fe ₃ O ₄ @PC	H ₂ O, K ₂ CO ₃ , 60 °C	120	67	40
2	C nanocomposite Pd	DMF-H ₂ O (2:1), K ₂ CO ₃ , 100 °C	90	97	41
3	Pd-Fe ₃ O ₄ @Alginate anionic polysaccharide	Ethanol, H ₂ O, K ₂ CO ₃ , 80 °C	90	94	42
4	Pd@ Agarose- Fe ₃ O ₄	PEG-200, K ₂ CO ₃ , 80–130 °C	30	97	43
5	Pd-AcAcAm-Fe ₃ O ₄ @ SiO ₂	DMF- H ₂ O (8:1), K ₂ CO ₃ , 80 °C	120	98	44
6	Maghemite-Pd	DMF-H ₂ O, K ₂ CO ₃ , 110 °C	60	90	45
7	Fe ₃ O ₄ @EDTA-Pd	H ₂ O-TBAB, K ₂ CO ₃ , 80 °C	180	94	46
8	Im-Phos-SiO ₂ @Fe ₃ O ₄ /Pd	EtOH:H ₂ O (1:1), K ₂ CO ₃ , 30 °C	5 hrs.	90	47
9	Pd-CoFe ₂ O ₄	Ethanol, Na ₂ CO ₃ , Reflux	12 hrs.	81	48
10	Pd/MnFe₂O₄	DMF:H₂O (1:1), K₂CO₃, 90°C	10	98	This work

**Fig. 7.** Optimization of bases for Suzuki cross-coupling.**Scheme 2.** Plausible mechanism of Suzuki cross-coupling.

3.2.3. Reusability of Pd/MnFe₂O₄ catalyst

Reusability is one of the emphasized features of green catalysts. After completion of reaction the catalyst was magnetically separated, washed with water and ethanol several times and dried for two hours in an oven. The resulting catalyst was employed for next reaction cycle of phenyl boronic acid and Bromobenzene. The catalyst recovered by same way and reused up to six reaction cycles. The results are summarized in Fig. 8. From the result it reveals that the catalytic activity of Pd/MnFe₂O₄ is admirable even after six runs. The structural stability of the catalyst after six runs have been also examined by XRD and EDS analysis, which is in good agreement with the results.

**Fig. 8.** Reusability of Pd/MnFe₂O₄ in model reaction.

3.2.4. Comparative study

The efficacy of synthesized Pd/MnFe₂O₄ catalyst was verified by comparing with reported palladium catalysts for the model reaction of phenyl boronic acid and Iodobenzene (Table 5). The comparative study revealed that the testified methods travail with factors like requirement of high temperature and low yield of product. However, Pd/MnFe₂O₄ catalyst was found to be superior with respect to time, yield, and reaction conditions [40–48].

4. Conclusion

In conclusion, a green and efficient Pd/MnFe₂O₄ nanocomposite was developed by citrate-gel auto combustion and deposition-precipitation method. The catalyst employed for the Suzuki cross coupling of aryl halides with boronic acid in aqueous medium. The

catalyst was well characterized by XRD, SEM, EDS, TEM, BET, and DLS analysis, which confirmed the coupling of Pd with MnFe₂O₄ nanosheets. Notably, the reaction required short time for formation of desired coupling product. The remarkable features of present method are short reaction time, high yield, use of aqueous solvent, high TON/TOF, easy magnetic separation and reusability of Pd/MnFe₂O₄ catalyst. The efficiency of catalyst was sustained even after six reaction cycles, which was confirmed by EDS and XRD analysis.

Selected spectral data of Suzuki cross-coupling reaction

Table 3, Entry 1, 7, 14: 1-1'-biphenyl [C₁₂H₁₀]

White solid, mp 70–72 °C (lit. 69–70 °C); ¹H NMR (400 MHz, CDCl₃), δ (ppm): 7.31–7.35 (m, 2H), 7.36–7.44 (m, 4H), 7.45–7.60 (m, 4H); ¹³C NMR (100 MHz, CDCl₃), δ (ppm): 127.41, 128.99, 141.51 ppm.

Table 3, Entry 3: 4-methoxy-3'-methyl-1-1'-biphenyl [C₁₄H₁₄O]

White solid, mp 52–54 °C (lit. 51–52 °C) ¹H NMR (400 MHz, CDCl₃), δ (ppm): 2.41 (s, 3H), 3.85 (s, 3H), 6.96–6.98 (m, 2H), 7.12–7.13 (m, 1H), 7.29–7.37 (m, 3H), 7.51–7.53 (m, 2H); ¹³C NMR (100 MHz, CDCl₃), δ (ppm): 17.75, 21.68, 29.06, 33.30, 55.33, 114.12, 123.83, 127.39, 127.55, 128.14, 128.60, 146.71, 168.39.

Table 3, Entry 8: 3-methoxy-1-1'-biphenyl [C₁₃H₁₂O]

White solid, mp 82–84 °C (lit. 81–82 °C) ¹H NMR (400 MHz, CDCl₃), δ (ppm): 3.85 (s, 3H), 6.87–6.90 (m, 1H), 7.11–7.12 (m, 1H), 7.16–7.18 (m, 1H), 7.31–7.36 (m, 2H), 7.40–7.44 (m, 2H), 7.56–7.59 (m, 2H); ¹³C NMR (100 MHz, CDCl₃), δ (ppm): 55.53, 112.94, 113.18, 119.93, 127.44, 127.64, 128.96, 129.97, 141.37, 143.04, 160.22.

Table 3, Entry 10: 4'-methoxy-[1-1'-biphenyl]-4-carbaldehyde [C₁₄H₁₂O₂]

White solid, mp 102–104 °C (lit. 101–102 °C) ¹H NMR (400 MHz, CDCl₃), δ (ppm): 3.87 (s, 3H), 6.99–7.03 (m, 2H), 7.58–7.61 (m, 2H), 7.71–7.73 (m, 2H), 7.91–7.94 (m, 2H), 10.04 (s, 1H); ¹³C NMR (100 MHz, CDCl₃), δ (ppm): 55.40, 114.46, 127.06, 128.50, 130.33, 132.05, 134.64, 146.79, 160.09, 191.94.

Table 3, Entry 12: 4-methoxy-4'-methyl-1-1'-biphenyl [C₁₄H₁₄O]

White solid, mp 110–112 °C (lit. 112 °C) ¹H NMR (400 MHz, CDCl₃), δ (ppm): 2.40 (s, 3H), 3.87 (s, 3H), 6.96–7.00 (m, 2H), 7.23–7.28 (m, 2H), 7.45–7.48 (m, 2H), 7.51–7.54 (m, 2H); ¹³C NMR (100 MHz, CDCl₃), δ (ppm): 21.07, 55.34, 113.47, 114.14, 125.76, 126.59, 126.97, 127.96, 129.44, 129.91, 130.25, 130.30, 133.73, 136.36, 137.95, 141.53, 158.91.

Declaration of Competing Interest

The authors declare that they have no known competing financial interests or personal relationships that could have appeared to influence the work reported in this paper.

CRediT authorship contribution statement

Damodar J. Sutar: Methodology, Data curation, Investigation, Writing – original draft. **Sunil N. Zende:** Supervision, Data curation, Investigation. **Abhijit N. Kadam:** Data curation, Investigation. **Mukund.G. Mali:** Supervision, Data curation, Investigation. **Pradeep M. Mhaldar:** Methodology, Data curation, Investigation. **Asmita.S. Tapase:** Data curation, Formal analysis. **Chinna Bathula:** Data curation, Formal analysis. **Sang-Wha Lee:** Methodology, Data curation, Formal analysis. **Gavisiddappa S. Gokavi:** Supervision, Methodology, Visualization, Investigation, Writing – review & editing.

Data Availability

No data was used for the research described in the article.

Acknowledgment

One of the authors, DJS is thankful to Mahatma Jyotiba Phule Research and Training Institute (Mahajyoti), Nagpur, Maharashtra, India, for financial support. GSG acknowledge the research facilities provided by Shivaji University, Kolhapur.

Supplementary materials

Supplementary material associated with this article can be found, in the online version, at doi:10.1016/j.jorgchem.2022.122541.

References

- [1] (a) N. Miyaura, A. Suzuki, Chem. Rev. 95 (1995) 2457, doi:10.1021/cr00039a007; (b) L. Yin, J. Liebscher, Chem. Rev. 107 (2007) 133–173, doi:10.1021/cr0505674.
- [2] (a) A.K. Diallo, C. Ornelas, L. Salmon, J.R. Aranzas, D. Astruc, Angew. Chem. Int. Ed. 119 (2007) 8798–8802, doi:10.1002/ange.200703067; (b) G. Altenhoff, R. Goddard, C.W. Lehmann, F. Glorius, Angew. Chem. Int. Ed. 42 (2003) 3690–3693, doi:10.1002/anie.200351325.
- [3] L. Djakovitch, K. Kohler, J.G. De Vries, in: Nanoparticles and Catalysis, Wiley-VCH, Weinheim, 2008, pp. 303–348. (Ed.: D. Astruc).
- [4] (a) O. Kitamura, S. Sako, T. Udzu, A. Tsutsui, T. Maegawa, Y. Monguchi, H. Sajiki, Chem. Commun. 47 (2007) 5069–5071, doi:10.1039/B712207A; (b) T. Itoha, H. Danjob, W. Sasaki, K. Urita, E. Bekyarovac, M. Araia, T. Imamoto, M. Yudasakad, S. Iijimad, H. Kanoha, K. Kanekoa, Carbon 46 (2008) 172–175, doi:10.1016/j.carbon.2007.10.026.
- [5] (a) D.H. Lee, J.H. Kim, B.H. Jun, H. Kang, J. Park, Y.S. Lee, Org. Lett. 10 (2008) 1609–1612, doi:10.1021/ol8003047; (b) S. Schweizer, J.-M. Becht, C.L. Drian, Org. Lett. 9 (2007) 3777–3780, doi:10.1021/ol701460z.
- [6] (a) C.M. Crudden, M. Sateesh, R. Lewis, J. Am. Chem. Soc. 127 (2005) 10045–10050, doi:10.1021/ja0430954; (b) M. Choi, D.H. Lee, K. Na, B.W. Yu, R. Ryoo, Angew. Chem. Int. Ed. 48 (2009) 3673–3676, doi:10.1002/anie.200806334; (c) S. MacQuarrie, B. Nohair, J.H. Horton, S. Kaliaguine, C.M. Crudden, J. Phys. Chem. 114 (2010) 57–64, doi:10.1021/jp908260j.
- [7] (a) M. Lysen, K. Kohler, Synlett 11 (2005) 1671–1674, doi:10.1055/s-2005-869877; (b) M. Lysen, K. Kohler, 4, (2006), 692–698, 10.1055/s-2006-926305; (c) M.J. Jin, D.H. Lee, Angew. Chem. Int. Ed. 49 (2010) 1119–1122, doi:10.1002/anie.200905626; (d) B.M. Choudary, S. Madhi, N.S. Chowdari, M.L. Kantam, B. Sreedhar, J. Am. Chem. Soc. 124 (2002) 14127–14136, doi:10.1021/ja026975w; (e) Y. Tsuji, T. Fujihara, Inorg. Chem. 46 (2007) 1895–1902, doi:10.1021/ic061872q.
- [8] S. Lincic, P. Christopher, D.B. Ingram, Nat. Mater. 10 (2011) 911–921, doi:10.1038/nmat3151.
- [9] E.M. Zahran, N.M. Bedford, M.A. Nguyen, Y.J. Chang, B.S. Guiton, R.R. Naik, L.G. Bachas, M.R. Knecht, J. Am. Chem. Soc. 136 (2014) 32–35, doi:10.1021/ja410465s.
- [10] Y. Yu, T. He, L. Guo, Y. Yang, L. Guo, Y. Tang, Y. Cao, Sci. Rep. 5 (9561) (2015) 1–7, doi:10.1038/srep09561.
- [11] R. Costi, G. Cohen, A. Salant, E. Rabani, U. Banin, Nano Lett. 9 (2009) 2031–2039, doi:10.1021/nl900301v.
- [12] A. Figuerola, A. Fiore, R. Di Corato, A. Falqui, C. Giannini, E. Micotti, A. Lascialfari, M. Corti, R. Cingolani, T. Pellegrino, P.D. Cozzoli, L. Manna, J. Am. Chem. Soc. 130 (2008) 1477–1487, doi:10.1021/ja078034v.
- [13] X.C. Ma, Y. Dai, L. Yu, B.B. Huang, Nature 5 (2016) e16017, doi:10.1038/lsa.2016.17.
- [14] M.S. El Deab, T. Ohsaka, Angew. Chem. Int. Ed. 45 (2006) 5963–5966, doi:10.1002/anie.200600692.
- [15] B. Gilbert, F. Huang, H. Zhang, G.A. Waychunas, J.F. Banfield, Science 305 (2004) 651–654, doi:10.1126/science.1098454.
- [16] W.J. Huang, R. Sun, J. Tao, L.D. Menard, R.G. Nuzzo, J.M. Zuo, Nat. Mater. 7 (2008) 308–313, doi:10.1038/nmat2132.
- [17] H. Yu, M. Chen, P.M. Rice, S.X. Wang, R.L. White, S. Sun, Nano Lett. 5 (2005) 379–382, doi:10.1021/nl047955q.
- [18] B. Aslibeiki, P. Kasmeri, J. Supercond. Nov. Magn. 28 (2015) 3343–3350, doi:10.1007/s10948-015-3154-y.
- [19] Y. Zhu, L.P. Stubbs, F. Ho, R. Liu, C.P. Ship, J.A. Maguire, N.S. Hosmane, Chem-CatChem 2 (2010) 365–374, doi:10.1002/cctc.200900314.
- [20] L. Zhang, Y. Wu, J. Nanomater. 2013 (2013) 1–6, doi:10.1155/2013/640940.
- [21] A.M. Jacinthia, V. Umamathy, P. Neeraja, S.R. Jeya Rajkumar, J. Nanostruct. Chem. 7 (2017) 375–387, doi:10.1007/s40097-017-0248-z.
- [22] U. Yenial, T. Abo Atia, G. Granata, I. Pettiti, F. Pagnanelli, J. Mol. Liq. 318 (2020) 1–10, doi:10.1016/j.molliq.2020.114047.
- [23] M. Rezaei, S.M. Mirkazemi, S. Alamolhoda, J. Supercond. Nov. Magn. 34 (2021) 1397–1408, doi:10.1007/s10948-021-05830-0.
- [24] R. Mozafari, F. Heidarzadeh, F. Nikpour, Mater. Sci. Eng. C 105 (2019) 1–12, doi:10.1016/j.msec.2019.110109.
- [25] R. Mozafari, F. Heidarzadeh, Polyhedron 162 (2019) 263–276, doi:10.1016/j.poly.2019.01.065.

- [26] G. Chen, X. Zhang, Y. Gao, G. Zhu, Q. Cheng, X. Cheng, Sep. Purif. Technol. 213 (2019) 456–464, doi:[10.1016/j.seppur.2018.12.049](https://doi.org/10.1016/j.seppur.2018.12.049).
- [27] K. Dhanalaxmi, R. Yadav, S.K. Kundu, B.M. Reddy, V. Amoli, A. Kumar Sinha, J. Mondal, Chem. Eur. J. 22 (2016) 15639–15644, doi:[10.1002/chem.201603419](https://doi.org/10.1002/chem.201603419).
- [28] Y. Rahmayeni, S. Arief, N. Jamarun, E. Emriadi, Y. Stiadi, Orient. J. Chem. 33 (2017) 2758–2765, doi:[10.13005/ojc/330608](https://doi.org/10.13005/ojc/330608).
- [29] M.C. D'Alterio, E. Casals-Cruañas, N.V. Tzouras, G. Talarico, S.P. Nolan, A. Poater, Chem. Eur. J. 27 (2021) 13481–13493, doi:[10.1002/chem.202101880](https://doi.org/10.1002/chem.202101880).
- [30] Yi-Luen Huang, Chia-Ming Weng, Fung-E. Hong, Chem. Eur. J. 14 (2008) 4426–4434, doi:[10.1002/chem.200800011](https://doi.org/10.1002/chem.200800011).
- [31] P.G. Kargar, G. Bagherzade, Front. Chem. 9 (2021) 1–19, doi:[10.3389/fchem.2021.747016](https://doi.org/10.3389/fchem.2021.747016).
- [32] R. Majumdar, S. Tantayanon, B.G. Bag, Int. Nano Lett. 7 (2017) 267–274, doi:[10.1007/s40089-017-0220-4](https://doi.org/10.1007/s40089-017-0220-4).
- [33] F. Wang, C. Li, H. Chen, R. Jiang, L. Sun, Q. Li, J. Wang, J.C. Yu, C. Yan, J. Am. Chem. Soc. 135 (2013) 5588–5601, doi:[10.1021/ja310501y](https://doi.org/10.1021/ja310501y).
- [34] T. Shanmugavel, S. Gokul Raj, G. Ramesh Kumar, G. Rajarajan, Phys. Procedia 54 (2014) 159–163, doi:[10.1016/j.phpro.2014.10.053](https://doi.org/10.1016/j.phpro.2014.10.053).
- [35] M. Zhu, G. Diao, J. Phys. Chem. 115 (2011) 24743–24749, doi:[10.1021/jp206116e](https://doi.org/10.1021/jp206116e).
- [36] M. Shirzadi-Ahodashi, M. Ebrahimzadeh, S. Ghoreishi, A. Naghizadeh, S. Mortazavi-Derazkola, Appl. Organomet. Chem. e5614 (2020) 1–12, doi:[10.1002/aoc.5614](https://doi.org/10.1002/aoc.5614).
- [37] Z. Wei, D. Wang, Y. Liu, X. Guo, Y. Zhu, Z. Meng, Z. Yu, W. Wong, J. Mater. Chem. 8 (2020) 10774–10780, doi:[10.1039/d0tc01380c](https://doi.org/10.1039/d0tc01380c).
- [38] J. Huang, K. Yung, G. Li, Z. Wei, Z. Meng, IEEE Magn. Lett. 10 (2019) 6101303, doi:[10.1109/LMAG.2019.2892930](https://doi.org/10.1109/LMAG.2019.2892930).
- [39] T. Ye, Y. Lu, Z. Xiao, J. Li, T. Nakao, H. Abe, Y. Niwa, M. Kitano, T. Tada, H. Hosono, Nat. Commun. 10 (2019) 1–10, doi:[10.1038/s41467-019-13679-0](https://doi.org/10.1038/s41467-019-13679-0).
- [40] A. Pourjavadi, Z. Hababi, Appl. Organomet. Chem. 32 (2018) 1–12, doi:[10.1002/aoc.4480](https://doi.org/10.1002/aoc.4480).
- [41] M. Shokouhimehr, T. Kim, S.W. Jun, K. Shin, Y. Jang, B. Hyo Kim, J. Kim, T. Hyeona, Appl. Catal. A Gen. 476 (2014) 133–139, doi:[10.1016/j.apcata.2014.02.029](https://doi.org/10.1016/j.apcata.2014.02.029).
- [42] R.S. Shelkar, S.H. Gund, J.M. Nagarkar, RSC Adv. 4 (2014) 53387–53396, doi:[10.1039/C4RA08726G](https://doi.org/10.1039/C4RA08726G).
- [43] H.F. Nasser Iranpoor, M. Gholinejad, S. Akbari, N. Jeddi, RSC Adv. 4 (2014) 17060–17070, doi:[10.1039/C4RA00900B](https://doi.org/10.1039/C4RA00900B).
- [44] S.P. Vibhute, P.M. Mhaldar, R. Sejwal, D.M. Pore, Tetrahedron Lett. 61 (2020) 1–11, doi:[10.1016/j.tetlet.2020.151594](https://doi.org/10.1016/j.tetlet.2020.151594).
- [45] A.K. Rathi, M.B. Gawande, J. Pechousek, J. Tucek, C. Aparicio, M. Petr, O. Tomanec, R. Krikavova, Z. Travnicek, R.S. Varma, R. Zboril, Green Chem. 18 (2016) 2363–2373, doi:[10.1039/C5GC02264A](https://doi.org/10.1039/C5GC02264A).
- [46] K. Azizi, E. Ghonchepour, M. Karimi, A. Heydari, Appl. Organomet. Chem. 29 (2015) 187–194, doi:[10.1002/aoc.3258](https://doi.org/10.1002/aoc.3258).
- [47] M. Gholinejad, M. Razeghi, A. Ghaderi, P. Biji, Catal. Sci. Technol. 6 (2016) 3117–3127, doi:[10.1039/C5CY00821B](https://doi.org/10.1039/C5CY00821B).
- [48] K. Senapati, S. Roy, C. Borgohain, P. Phukan, J. Mol. Catal. A Chem. 352 (2012) 128–134, doi:[10.1016/j.molcata.2011.10.022](https://doi.org/10.1016/j.molcata.2011.10.022).